Journal of Machine Learning Research 19 (2018) 1-30 Submitted 11/17; Revised 8/18; Published 10/18

Extrapolating Expected Accuracies for Large Multi-Class Problems

Charles Zheng CHARLES.Y.ZHENG@GMAIL.COM
Section on Functional Imaging Methods
National Institute of Mental Health
Bethesda, MD

Rakesh Achanta RAKESHA@STANFORD.EDU
Department of Statistics
Stanford University
Palo Alto, CA

Yuval Benjamini YUVAL.BENJAMINI@MAIL.HUJI.AC.IL
Department of Statistics
The Hebrew University of Jerusalem,
Jerusalem, Israel

Editor: Christoph Lampert

Abstract

The difficulty of multi-class classification generally increases with the number of classes. Using data for a small set of the classes, can we predict how well the classifier scales as the number of classes increases? We propose a framework for studying this question, assuming that classes in both sets are sampled from the same population and that the classifier is based on independently learned scoring functions. Under this framework, we can express the classification accuracy on a set of k classes as the $(k-1)$st moment of a discriminability function; the discriminability function itself does not depend on k. We leverage this result to develop a non-parametric regression estimator for the discriminability function, which can extrapolate accuracy results to larger unobserved sets. We also formalize an alternative approach that extrapolates accuracy separately for each class, and identify tradeoffs between the two methods. We show that both methods can accurately predict classifier performance on label sets up to ten times the size of the original set, both in simulations as well as in realistic face recognition or character recognition tasks.

Keywords: Multi-class problems, face recognition, object recognition, transfer learning, nonparametric models

1. Introduction

Many machine learning tasks are interested in recognizing or identifying an individual instance within a large set of possible candidates. These problems are usually modeled as multi-class classification problems, with a large and possibly complex label set. Leading examples include detecting the speaker from his voice patterns (Togneri and Pullella, 2011), identifying the author from her written text (Stamatatos et al., 2014), or labeling the object category from its image (Duygulu et al., 2002; Deng et al., 2010; Oquab et al., 2014). In

all these examples, the algorithm observes an input x, and uses the classifier function h to guess the label y from a large label set $\mathcal{S}$.

There are multiple practical challenges in developing classifiers for large label sets. Collecting high quality training data is perhaps the main obstacle, as the costs scale with the number of classes. It can be more affordable to first collect data for a small set of classes, even if the long-term goal is to generalize to a larger set. Furthermore, classifier development can be accelerated by training first on fewer classes, as each training cycle may require substantially less resources. Indeed, due to interest in how small-set performance generalizes to larger sets, such comparisons can found in the literature (Oquab et al., 2014; Griffin et al., 2007). A natural question is: how does changing the size of the label set affect the classification accuracy?

We consider a pair of classification problems on finite label sets: a source task with label set $\mathcal{S}_{k_1}$ of size k_1, and a target task with a larger label set $\mathcal{S}_{k_2}$ of size $k_2 > k_1$. For each label set $\mathcal{S}_k$, one constructs the classification rule $h^{(k)} : \mathcal{X} \to \mathcal{S}_k$. Supposing that in each task, the test example (X^*, Y^*) has a joint distribution, define the generalization accuracy for label set $\mathcal{S}_k$ as

$$\mathrm{GA}_k = \Pr[h^{(k)}(X^*) = Y^*]. \tag{1}$$

The problem of *performance extrapolation* is the following: using data from only the source task $\mathcal{S}_{k_1}$, predict the accuracy for a target task with a larger unobserved label set $\mathcal{S}_{k_2}$.

A natural use case for performance extrapolation would be in the deployment of a facial recognition system. Suppose a system was developed in the lab on a database of k_1 individuals. Clients would like to deploy this system on a new larger set of k_2 individuals. Performance extrapolation could allow the lab to predict how well the algorithm will perform on the clients' problem, accounting for the difference in label set size.

Extrapolation should be possible when the source and target classifications belong to the same problem domain. In many cases, the set of categories $\mathcal{S}$ is to some degree a random or arbitrary selection out of a larger, perhaps infinite, set of potential categories $\mathcal{Y}$. Yet any specific experiment uses a fixed finite set. For example, categories in the classical Caltech-256 image recognition data set (Griffin et al., 2007) were assembled by aggregating keywords proposed by students and then collecting matching images from the web. The arbitrary nature of the label set is even more apparent in biometric applications (face recognition, authorship, fingerprint identification) where the labels correspond to human individuals (Togneri and Pullella, 2011; Stamatatos et al., 2014). In all these cases, the number of the labels used to define a concrete data set is therefore an experimental choice rather than a property of the domain. Despite the arbitrary nature of these choices, such data sets are viewed as representing the larger problem of recognition within the given domain, in the sense that success on such a data set should inform performance on similar problems.

In this paper, we assume that both $\mathcal{S}_{k_1}$ and $\mathcal{S}_{k_2}$ are samples consisting of independent and identically distributed (i.i.d.) labels from a population (or prior distribution) π, which is defined on the label space $\mathcal{Y}$. We have no constraints on the dependence between $\mathcal{S}_{k_1}$ and $\mathcal{S}_{k_2}$: for example, $\mathcal{S}_{k_1}$ may be independent of $\mathcal{S}_{k_2}$, or alternatively $\mathcal{S}_{k_1}$ may be a subsample of $\mathcal{S}_{k_2}$ (the latter case is used in our experiments in Section 5). The sampling assumption is an approximate characterization of the label selection process, which is often at least partially manual. Nevertheless, it provides the exact properties we need without having

to derive specialized metrics of how similar $\mathcal{S}_{k_2}$ is to $\mathcal{S}_{k_1}$. This simplifies the theory, and demonstrates that in a very general setting, extrapolation is possible. We also make the assumption that the classifiers train a model independently for each class. This convenient property allows us to characterize the accuracy of the classifier by selectively conditioning on one class at a time.

Since we assume the label set is random, the generalization accuracy of a given classifier becomes a random variable. Performance extrapolation then becomes the problem of estimating the average generalization accuracy AGA_k of an i.i.d. label set $\mathcal{S}_k$ of size k. Roughly speaking, the achievable accuracy of a classification problem depends on how well the labels can be 'separated' based on the training data– that is, how different the empirical distributions of the training data look at the points where new test instances are drawn. The condition of i.i.d. sampling of labels ensures that the separation of labels in a random set $\mathcal{S}_{k_2}$ can be inferred by looking at the empirical separation in $\mathcal{S}_{k_1}$, and therefore that some estimate of the average accuracy on $\mathcal{S}_{k_2}$ can be obtained.

Our paper presents several main contributions related to extrapolation within this framework. First, we present a theoretical formula describing how average accuracy for smaller k is linked to average accuracy for label set of size $K > k$. We show that accuracy at any size depends on a discriminability function D, which is determined by properties of the data distribution and the classifier but does not depend on k. Second, we propose an estimation procedure that allows extrapolation of the observed average accuracy curve from k_1-class data to a larger number of classes, based on the theoretical formula. Under certain conditions, the estimation method has the property of being an unbiased estimator of the average accuracy. Third, we formalize an alternative approach (proposed by Kay et al. (2008)) that extrapolates accuracy separately for each class, and discuss tradeoffs between the two methods.

The paper is organized as follows. In the rest of this section, we discuss related work. The framework of randomized classification is introduced in Section 2, and there we also introduce a toy example which is revisited throughout the paper. Section 3 develops our theory of extrapolation, and in Section 3.3 we suggest an estimation method. We evaluate our method using simulations in Section 4. In Section 5, we demonstrate our method on a facial recognition problem, as well as an optical character recognition problem. In Section 6 we discuss modeling choices and limitations of our theory, as well as potential extensions.

1.1. Related Work

Linking performance between two different but related classification tasks can be considered an instance of transfer learning (Pan and Yang, 2010). Under Pan and Yang's terminology, our setup is an example of multi-task learning, because the source task has labeled data, which is used to predict performance on a target task that also has labeled data. Applied examples of transfer learning from one label set to another include Oquab et al. (2014), Donahue et al. (2014), Sharif Razavian et al. (2014). However, there is little theory for predicting the behavior of the learned classifier on a new label set. Instead, most research of classification for large label sets deal with the computational challenges of jointly optimizing the many parameters required for these models for specific classification algorithms (Crammer and Singer, 2001; Lee et al., 2004; Weston and Watkins, 1999). Gupta et al.

(2014) presents a method for estimating the accuracy of a classifier which can be used to improve performance for general classifiers, but doesn't apply for different set sizes.

The theoretical framework we adopt is one where there exists a family of classification problems with increasing number of classes. This framework can be traced back to Shannon (1948), who considered the error rate of a random codebook, which is a special case of randomized classification. More recently, a number of authors have considered the problem of high-dimensional feature selection for multi-class classification with a large number of classes (Pan et al., 2016; Abramovich and Pensky, 2015; Davis et al., 2011). All of these works assume specific distributional models for classification compared to our more general setup. However, we do not deal with the problem of feature selection.

Perhaps the most similar method that deals with extrapolation of classification error to a larger number of classes can be found in Kay et al. (2008). They trained a classifier for identifying the observed stimulus from a functional MRI scan of brain activity, and were interested in its performance on larger stimuli sets. They proposed an extrapolation algorithm, based on per-class kernel density estimation, as a heuristic with little theoretical discussion. In Section 3.5, we formalize their method within our framework, and implement two variations of their algorithm. We present simulation results and theoretical arguments to compare the algorithm to the regression approach we propose.

2. Randomized Classification

The randomized classification model we study has the following features. We assume that there exists an infinite, perhaps continuous, label space $\mathcal{Y}$ and an example space $\mathcal{X} \subseteq \mathbb{R}^p$. In the subsequent theory we assume that $\mathcal{Y}$ is continuous solely for the sake of mathematical convenience, so that we can discuss probability integrals on the space without the use of measure-theoretic notation. However, the theory would also approximately describe the case of $\mathcal{Y}$ is a sufficiently large discrete space, as long as the probability mass of the largest atom is suitably small.

We assume there exists a prior distribution π on the label space $\mathcal{Y}$, and that for each label $y \in \mathcal{Y}$, there exists a distribution of examples F_y. In other words, for an example-label pair (X, Y), the conditional distribution of X given $Y = y$ is given by F_y.

A random classification task can be generated as follows. The label set $\mathcal{S} = \{Y^{(1)}, \ldots, Y^{(k)}\}$ is generated by drawing labels $Y^{(1)}, \ldots, Y^{(k)}$ i.i.d. from π. Here we assume the number of labels k to be deterministic. For each label, we sample a training set and a test set. The test set is obtained by sampling r observations $X_\ell^{(i)}$ i.i.d. from $F_{Y^{(i)}}$ for $\ell = 1, \ldots, r$. For now, we can also assume that the training set is obtained by sampling r_{train} observations $X_{\ell,train}^{(i)}$ i.i.d. from $F_{Y^{(i)}}$ for $\ell = 1, \ldots, r_{train}$ and $i = 1, \ldots, k$. However, later we will relax these assumptions on the sampling of the training sets, so that we can accommodate classes have differing or stochastically determined number of instances, as long as the number of training instances for different labels are conditionally independent.

Recalling the face recognition example, $\mathcal{Y}$ is the space of all people, π is some distribution for sampling over people, X is a photo of a person's face, and F_Y is the conditional distribution of photos for person Y. The goal of classification is to label the photo X with the correct person Y.

We assume that the classifier $h(x)$ works by assigning a score to each label $y^{(i)} \in \mathcal{S}$, then choosing the label with the highest score. That is, there exist real-valued *score functions* $m_{y^{(i)}}(x)$ for each label $y^{(i)} \in \mathcal{S}$. Here we used the lower-case notation $y^{(i)}$ for the labels, treating them as fixed for now. Since the classifier is allowed to depend on the training data, it is convenient to view it (and its associated score functions) as random. We write $H(x)$ when we wish to work with the classifier as a random function, and likewise $M_y(x)$ to denote the score functions whenever they are considered as random. Since the classifier works by choosing the label with the highest score, the classifier is correct for a given test instance x^* with true label y^* whenever $m_{y^*}(x^*) = \max_j m_{y^{(j)}}(x^*)$, assuming that there are no ties.

For a fixed instance of the classification task with labels $\mathcal{S} = \{y^{(i)}\}_{i=1}^k$ and associated score functions $\{m_{y^{(i)}}\}_{i=1}^k$, recall the definition of the k-class generalization error (1). We will use the assumption that the test labels are uniformly distributed[1] over $\mathcal{S}$, which makes $\mathrm{GA}_k(h, \mathcal{S})$ a *balanced accuracy*, which equally weights the accuracies of the individual classes. Assuming that there are no ties, it can be written in terms of score functions as

$$\mathrm{GA}_k(h, \mathcal{S}) = \frac{1}{k} \sum_{i=1}^{k} \Pr[m_{y^{(i)}}(X^{(i)}) = \max_j m_{y^{(j)}}(X^{(i)})],$$

where $X^{(i)} \sim F_{y^{(i)}}$ for $i = 1, \ldots, k$.

However, it is often appropriate to model the labels $\{Y^{(i)}\}_{i=1}^k$ as a random sample from a distribution. Examples for such *randomized classification* problems include face recognition, where faces are drawn from a larger population, and large multi-class problems where only an arbitrary subset of labels have been collected.

Given our assumption that k is fixed, a natural target for prediction extrapolation is the expected value of the generalization accuracy $\mathrm{GA}_k(h, \mathcal{S})$ over the distribution of label sets. We call this the k-class *average generalization accuracy* of the classifier, denoted AGA_k, and formally defined as

$$\begin{aligned}
\mathrm{AGA}_k &= \mathbf{E}[\mathrm{GA}_k(H, \mathcal{S}_k)] \\
&= \frac{1}{k} \sum_{i=1}^{k} \Pr[M_{Y^{(i)}}(X^{(i)}) = \max_j M_{Y^{(j)}}(X^{(i)})] \\
&= \Pr[M_Y(X) > \max_{j=1}^{k-1} M_{Y^{(j)}}(X)]
\end{aligned}$$

where $Y^{(1)}, \ldots, Y^{(k)} \overset{iid}{\sim} \pi$, and where (X, Y) is an independent draw with the same joint distribution as its superscripted counterparts $(X^{(i)}, Y^{(i)})$. The last line follows from noting that all k summands in the previous line are identical, as each $Y^{(i)}$ is drawn from the same distribution π. The definition of average generalization accuracy is illustrated in Figure 1.

Note that in this framework, the role of the training and test sets is different than how they are usually used machine learning. Our goal is to predict the accuracy achieved on another (random) label set. Therefore, both the training and test data may be used

1. In Section 6, we discuss extensions of our framework that can accommodate the case that the test labels are not uniformly drawn from $\mathcal{S}$, i.e. that one has a non-uniform prior distribution over test labels.

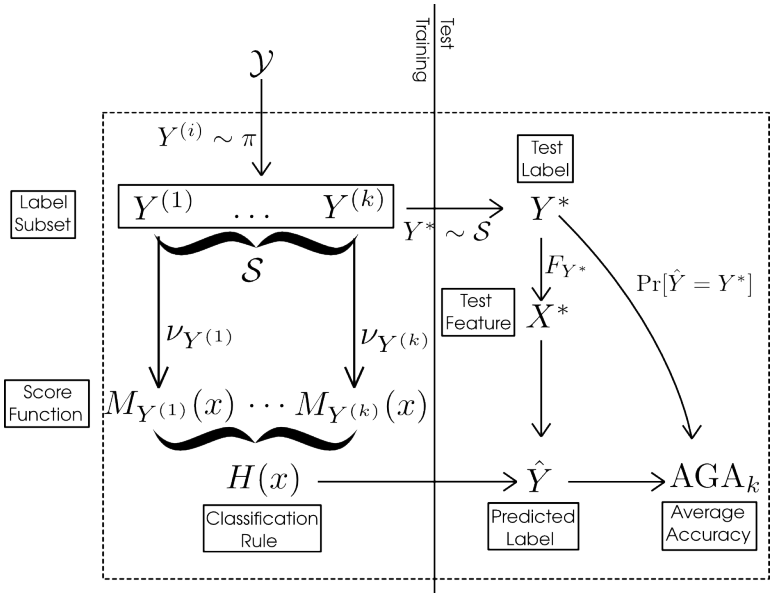

Figure 1: **Average generalization accuracy:** A diagram of the random quantities underlying the average generalization accuracy for k labels (AGA_k). At the training stage (left), a set of k labels $\mathcal{S}$ is sampled from the prior π, and score functions are trained from examples for these classes. At the test stage (right), one true class Y^* is sampled uniformly from $\mathcal{S}$, as well as a test example X^*. AGA_k measures the expected accuracy over these random variables.

in this estimation. Our approach, to be described in Section 2.3, uses the training data exclusively to construct classifiers on label subsets, and test data exclusively to estimate the distribution of favorability over test examples.

2.1. Marginal Classifier

The theoretical analysis of the average generalization accuracy is made much simpler if we can assume that the learning of the scoring functions $M_{Y^{(i)}}$ occurs independently for each labels–that is, there is no information shared between classes. For example, if there exists some function g such that

$$M_{y^{(i)}}(x) = g(x; y^{(i)}, (X^{(i)}_{1,train}, ..., X^{(i)}_{r_{train},train})),$$

the H is a marginal classifier since $M_{y^{(i)}}(x)$ only depends on the label $y^{(i)}$ and the class training set $X^{(i)}_{j,train}$.

In our analysis however, we shall relax the assumption that the classifier $H(x)$ is based on a training set[2]. Instead, it is sufficient that the score functions $\{M_{Y^{(i)}}\}_{i=1}^k$ associated

2. Due to this abstraction, our framework can accommodate scenarios where the classes have differing or stochastically determined number of instances, as long as the number of training instances for different labels are conditionally independent.

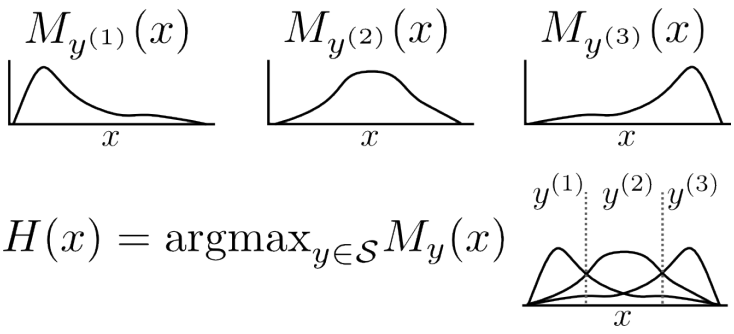

Figure 2: **Classification rule:** Top: Score functions for three classes in a one-dimensional example space. Bottom: The classification rule chooses between $y^{(1)}, y^{(2)}$ or $y^{(3)}$ by choosing the maximal score function.

with the random label set $\{Y^{(i)}\}_{i=1}^{k}$ are independent of the test instances. Under this formalism, we define a marginal classifier as follows.

Definition 1 *The classifier $H(x)$ is called a* marginal classifier *if and only if $M_{Y^{(i)}}$ are independent of both $Y^{(j)}$ and $M_{Y^{(j)}}$ for $j \neq i$.*

In marginal classifiers, classes "compete" only through selecting the highest score, but not in constructing the score functions. Therefore, each M_y can be considered to have been independently drawn from a distribution ν_y. The operation of a marginal classifier is illustrated in Figure 2.

For marginal classifiers, we can prove especially strong results about the accuracy of the classifier under i.i.d. sampling assumptions. And as we will see in the following section, many well-known types of classifiers satisfy the marginal property.

2.2. Examples of Marginal Classifiers

Estimated Bayes classifiers are primary examples of marginal classifiers. By this, we mean classifiers which output the class that maximizes the posterior probability for a class label according to Bayes' rule, but substituting in estimated distributions for the unknown true distributions. Let $\hat{f}_y$ be a density estimate of the example distribution under label y obtained from the empirical distribution $\hat{F}_y$, and let $\pi(y)$ be the prior distribution over labels. Then, we can use the estimated density to produce the score functions:

$$M_y^{EB}(x) = \log(\hat{f}_y(x)) + \log(\pi(y)).$$

The resulting empirical approximation for the Bayes classifier would be

$$H^{EB}(x) = \text{argmax}_{Y \in \mathcal{S}}(M_Y^{EB}(x)).$$

Both Quadratic Discriminant Analysis (QDA) and naïve Bayes classifiers can be seen as specific instances of an estimated Bayes classifier. For QDA, the score function is given by

$$m_y^{QDA}(x) = -(x - \mu(\hat{F}_y))^T \Sigma(\hat{F}_y)^{-1}(x - \mu(\hat{F}_y)) - \log\det(\Sigma(\hat{F}_y)),$$

where $\mu(F) = \int y dF(y)$ and $\Sigma(F) = \int (y - \mu(F))(y - \mu(F))^T dF(y)$. Hence, QDA is the special case of the estimated Bayes classifier when $\hat{f}_y$ is obtained as the multivariate Gaussian density with mean and covariance parameters estimated from the data.

In Naïve Bayes, the score function is

$$m_y^{NB}(x) = \sum_{j=1}^{p} \log \hat{f}_{y,j}(x),$$

where $\hat{f}_{y,j}$ is a density estimate for the j-th component of $\hat{F}_y$. Hence, Naïve Bayes is the estimated Bayes classifier when $\hat{f}_y$ is obtained as the product of estimated componentwise marginal distributions of $p(x_i|y)$.

For some classifiers, M_y is a deterministic function of y (and therefore ν_y is degenerate). A prime example is when there exist fixed or pre-trained embeddings $g, \tilde{g}$ that map both labels y and examples x into R^p. Then

$$M_y^{embed} = -\|g(y) - \tilde{g}(x)\|_2. \tag{2}$$

This would be the case when features from publicly available embeddings (e.g. word embedding vectors) are used for classification; see our example in Section 5. See also Pereira et al. (2018) for an example using word embedding vectors. Note that if the embeddings g or $\tilde{g}$ are informed by the specific set of classes in the experiment, this would no longer be a marginal classifier.

There are many classifiers which do not satisfy the marginal property, such as multinomial logistic regression, multilayer neural networks, decision trees, and k-nearest neighbors.

2.3. Estimation of Average Accuracy

Before tackling extrapolation, it will be useful for us to discuss the simpler task of generalizing accuracy results when the target set is *not* larger than the source set. This allows us to introduce several concepts and notations that are used in the harder problem of generalizing to a larger set. We will also illustrate all of these concept in a toy example following this section, which we shall revisit once more while tackling the problem of extrapolation.

Suppose we have training and test data for a classification task with k_1 classes. That is, we have a label set $\mathcal{S}_{k_1} = \{y^{(i)}\}_{i=1}^{k_1}$, and we assume that the training data has been used to obtain its associated set of score functions $M_{y^{(i)}}$. The test set, composed of $(x_1^{(i)}, \ldots, x_r^{(i)})$ for $i = 1, \ldots, k_1$ is also available to be used for this estimation task. What would be the predicted accuracy for a new randomly sampled set of $k_2 \leq k_1$ labels?

Note that AGA_{k_2} is the expected value of the accuracy on the new set of k_2 labels. Therefore, any unbiased estimator of AGA_{k_2} will be an unbiased predictor for the accuracy on the new set.

Let us start with the case $k_2 = k_1 = k$. For each test observation $x_\ell^{(i)}$, define the ranks of the candidate classes $j = 1, \ldots, k$ by

$$R_\ell^{i,j} = \sum_{s=1}^{k} I\{m_\ell^{(i,j)} \geq m_\ell^{(i,s)}\}.$$

where we have defined $m_\ell^{(i,j)} = m_{y^{(j)}}(x_\ell^{(i)})$. The test accuracy is the fraction of observations for which the correct class also has the highest rank

$$\mathrm{TA}_k = \frac{1}{rk}\sum_{i=1}^{k}\sum_{\ell=1}^{r} I\{R_\ell^{i,i} = k\}. \tag{3}$$

Taking expectations over both the test set and the random labels, the expected value of the test accuracy is AGA_k. Therefore, in this special case, TA_k provides an unbiased estimator for AGA_{k_2}.

Next, let us consider the case where $k_2 < k_1$. Consider label set $\mathcal{S}_{k_2}$ obtained by sampling k_2 labels uniformly without replacement from $\mathcal{S}_{k_1}$. Since $\mathcal{S}_{k_2}$ is unconditionally an i.i.d. sample from the population of labels π, the test accuracy of $\mathcal{S}_{k_2}$ is an unbiased estimator of AGA_{k_2}. However, we can get a better unbiased estimate of AGA_{k_2} by averaging over all the possible subsamples $\mathcal{S}_{k_2} \subset \mathcal{S}_{k_1}$. This defines the average test accuracy over subsampled tasks, ATA_{k_2}.

Remark. Naïvely, computing ATA_{k_2} requires us to train and evaluate $\binom{k_1}{k_2}$ classification rules. However, for marginal classifiers, retraining the classifier is not necessary. The rank $R_\ell^{i,i}$ of the correct label i for $x_\ell^{(i)}$, allows us to determine how many subsets $\mathcal{S}_2$ will result in a correct classification. Specifically, there are $R_\ell^{i,i} - 1 \leq k_2$ labels with a lower score than the correct label i. Therefore, as long as one of the classes in $\mathcal{S}_2$ is i, and the other $k_2 - 1$ labels are from the set of $R_\ell^{i,i} - 1$ labels with lower score than i, the classification of $x_j^{(i)}$ will be correct. This implies that there are $\binom{R_\ell^{i,i}-1}{k_2-1}$ such subsets $\mathcal{S}_2$ where $x_\ell^{(i)}$ is classified correctly, and therefore the average test accuracy for all $\binom{k_1}{k_2}$ subsets $\mathcal{S}_2$ is

$$\mathrm{ATA}_{k_2} = \frac{1}{\binom{k_1}{k_2}}\frac{1}{rk_2}\sum_{i=1}^{k_1}\sum_{\ell=1}^{r}\binom{R_\ell^{i,i}-1}{k_2-1}. \tag{4}$$

2.4. Toy Example: Bivariate Normal

Let us illustrate these ideas using a toy example. Let (Y, X) have a bivariate normal joint distribution,

$$(Y, X) \sim N\left(\begin{pmatrix}0\\0\end{pmatrix}, \begin{pmatrix}1 & \rho\\ \rho & 1\end{pmatrix}\right),$$

as illustrated in Figure 3(a). Therefore, for a given randomly drawn label Y, the conditional distribution of X for that label is univariate normal with mean ρY and variance $1 - \rho^2$,

$$X|Y = y \sim N(\rho y, 1 - \rho^2).$$

Supposing we draw $k = 3$ labels $\{y^{(1)}, y^{(2)}, y^{(3)}\}$, the classification problem will be to assign a test instance X^* to the correct label. The test instance X^* would be drawn with equal probability from one of three conditional distributions $X|Y = y^{(i)}$, as illustrated in Figure 3(b, top). The Bayes rule assigns X^* to the class with the highest density $p(x|y^{(i)})$, as illustrated by Figure 3(b, bottom): it is therefore a marginal classifier, with score function

$$M_y(x) = \log(p(x|y)) = -\frac{(x - \rho y)^2}{2(1 - \rho^2)} + \text{const.}$$

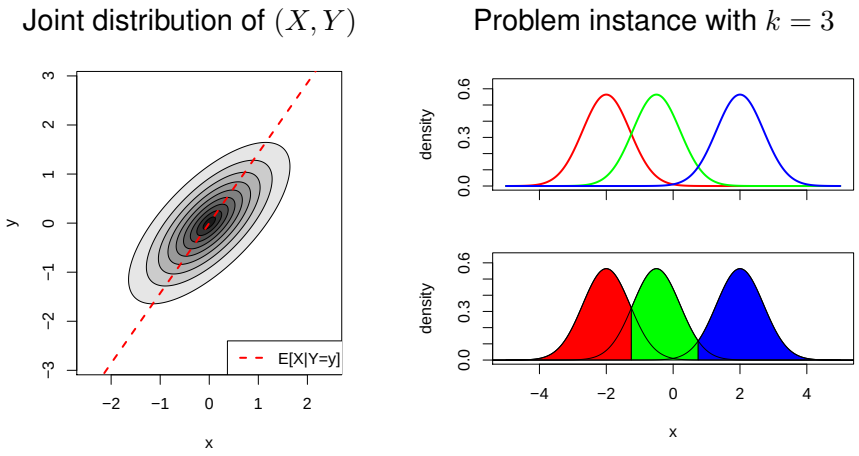

(a) (b)

Figure 3: **Toy example:** *Left:* The joint distribution of (X, Y) is bivariate normal with correlation $\rho = 0.7$. *Right:* A typical classification problem instance from the bivariate normal model with $k = 3$ classes. *(Top):* the conditional density of X given label Y, for $Y = \{y^{(1)}, y^{(2)}, y^{(3)}\}$. *(Bottom):* the Bayes classification regions for the three classes.

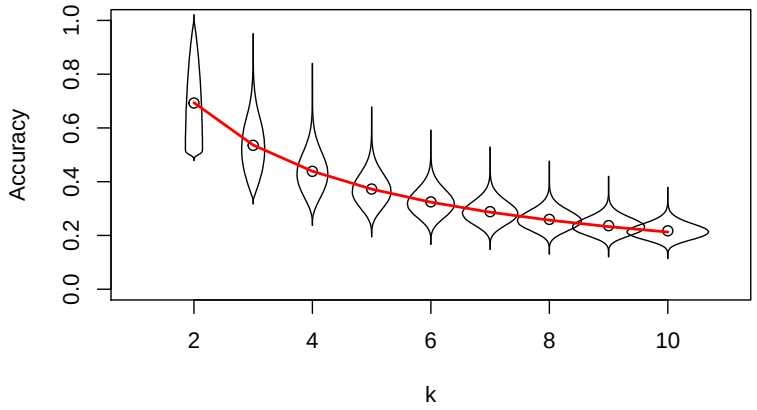

Figure 4: **Generalization accuracy for toy example:** The distribution of the generalization accuracy for $k = 2, 3, \ldots, 10$ for the bivariate normal model with $\rho = 0.7$. Circles indicate the average generalization accuracy AGA_k; the red curve is the theoretically computed average accuracy.

For this model, the generalization accuracy of the Bayes rule for any label set $\{y^{(1)}, \ldots, y^{(k)}\}$ is given by

$$\begin{aligned}\mathrm{GA}_k(h, \{y^{(1)}, \ldots, y^{(k)}\}) &= \frac{1}{k}\sum_{i=1}^{k} \Pr_{X \sim p(x|y^{(i)})}[p(X|y^{(i)}) = \max_{j=1}^{k} p(X|y^{(j)})] \\ &= \frac{1}{k}\sum_{i=1}^{k} \Phi\left(\frac{y^{[i+1]} - y^{[i]}}{2\sqrt{1-\rho^2}}\right) - \Phi\left(\frac{y^{[i-1]} - y^{[i]}}{2\sqrt{1-\rho^2}}\right),\end{aligned}$$

where Φ is the standard normal cdf, $y^{[1]} < \cdots < y^{[k]}$ are the sorted labels, $y^{[0]} = -\infty$ and $y^{[k+1]} = \infty$, and h is the maximum-margin classifier $h(x) = \mathrm{argmax}_{y \in \{y^{(1)}, \ldots, y^{(k)}\}} m_y(x)$. We numerically computed $\mathrm{GA}_k(h, \{Y^{(1)}, \ldots, Y^{(k)}\})$ for randomly drawn labels $Y^{(1)}, \ldots, Y^{(k)} \overset{iid}{\sim} N(0,1)$, and the distributions of GA_k for $k = 2, \ldots, 10$ are illustrated in Figure 4. The mean of the distribution of GA_k is the k-class average accuracy, AGA_k. The theory presented in the next section deals with how to analyze the average accuracy AGA_k as a function of k.

3. Extrapolation

The section is organized as follows. We begin by introducing an explicit formula for the average accuracy AGA_k. The formula reveals that AGA_k is determined by moments of a one-dimensional function $D(u)$. Using this formula, we can estimate $D(u)$ using subsampled accuracies. These estimates allow us to extrapolate the average generalization accuracy to an arbitrary number of labels.

The result of our analysis is to expose the average accuracy AGA_k as the weighted average of a function $D(u)$, where $D(u)$ is independent of k, and where k only changes the weighting.

One of the assumptions we rely on is the *tie-breaking condition*, which allows us to neglect specifying the case when margins are tied.

Definition 2 Tie-breaking condition*: for all $x \in \mathcal{X}$, $M_Y(x) \neq M_{Y'}(x)$ with probability one for Y, Y' independently drawn from π.*

In practice, one can simply break ties randomly, which is mathematically equivalent to adding a small amount of random noise ϵ to the function M.

The result is stated as follows.

Theorem 3 *Suppose π, $\{F_y\}_{y \in \mathcal{Y}}$, and score functions M_y satisfy the tie-breaking condition. Then, there exists a cumulative distribution function $D(u)$ defined on the interval $[0,1]$ such that*

$$AGA_k = 1 - (k-1)\int_0^1 D(u)u^{k-2}du. \tag{5}$$

3.1. Analysis of Average Accuracy

Recall that for marginal classifiers, the model M_Y should be independent of the other labels and independent of the test instances. We often consider a random label (Y) with its

associated score function (M_Y) and an example vector (X) drawn from label Y. Explicitly, this sampling can be written:

$$Y \sim \pi, \quad M_Y|Y \sim \nu_Y, \quad X|Y \sim F_Y.$$

Similarly we use $(Y', M_{Y'}, X')$ and (Y^*, M_{Y^*}, X^*) for two more triplets with independent and identical distributions. Specifically, X^* will typically note the test example, and therefore Y^* the true label and M_{Y^*} its score function.

The function D is related to a favorability function. Favorability measures the probability that the score for the example x is going to be maximized by a particular score function m_y, compared to a random competitor $M_{Y'}$. Formally, we write

$$U_x(m_y) = \Pr[m_y(x) > M_{Y'}(x)]. \tag{6}$$

Note that for fixed example x, favorability is monotonically increasing in $m_y(x)$. If $m_y(x) > m_{y^\dagger}(x)$, then $U_x(y) > U_x(y^\dagger)$, because the event $\{m_y(x) > M_{Y'}(x)\}$ contains the event $\{m_{y^\dagger}(x) > M_{Y'}(x)\}$.

Therefore, given labels $y^{(1)}, \ldots, y^{(k)}$ and test instance x, we can think of the classifier as choosing the label with the greatest favorability:

$$\hat{y} = \text{argmax}_{y^{(i)} \in \mathcal{S}} m_{y^{(i)}}(x) = \text{argmax}_{y^{(i)} \in \mathcal{S}} U_x(m_{y^{(i)}}).$$

Furthermore, via a conditioning argument, we see that this is still the case even when the test instance and labels are random, as long as the random example X^* is independent of Y. (Recall that in our notation, X and Y are dependent, but $X^* \perp Y$.)

$$\hat{Y} = \text{argmax}_{Y^{(i)} \in \mathcal{S}} M_{Y^{(i)}}(X^*) = \text{argmax}_{Y^{(i)} \in \mathcal{S}} U_{X^*}(M_{Y^{(i)}}).$$

The favorability takes values between 0 and 1, and when any of its arguments are random, it becomes a random variable with a distribution supported on $[0, 1]$. In particular, we consider the following two random variables:

a. the *incorrect-label* favorability $U_{x^*}(M_Y)$ between a given fixed test instance x^*, and the score function of a random incorrect label M_Y, and

b. the *correct-label* favorability $U_{X^*}(M_{Y^*})$ between a random test instance X^*, and the score function of the correct label, M_{Y^*}.

3.1.1. Incorrect-Label Favorability

The incorrect-label favorability can be written explicitly as

$$U_{x^*}(M_Y) = \Pr[M_Y(x^*) > M_{Y'}(x^*)|M_Y(x^*)]. \tag{7}$$

Note that M_Y and $M_{Y'}$ are identically distributed, and both are unrelated to x^* that is fixed. This leads to the following result:

Lemma 4 *Under the tie-breaking condition, the incorrect-label favorability $U_{x^*}(M_Y)$ is uniformly distributed for any $x^* \in \mathcal{X}$, meaning*

$$\Pr[U_{x^*}(M_Y) \leq u] = u \tag{8}$$

for all $u \in [0, 1]$.

Proof Write $U_{x^*}(M_Y) = \Pr[Z > Z'|Z]$, where $Z = M_Y(x)$ and $Z' = M_{Y'}(x)$ for $Y, Y' \overset{i.i.d.}{\sim} \pi$. The tie-breaking condition implies that $\Pr[Z = Z'] = 0$. Now observe that for independent random variables Z, Z' with $Z \overset{D}{=} Z'$ and $\Pr[Z = Z'] = 0$, the conditional probability $\Pr[Z > Z'|Z]$ is uniformly distributed. ■

3.1.2. Correct-Label Favorability

The correct-label favorability is

$$U^* = U_{X^*}(M_{Y^*}) = \Pr[M_{Y^*}(X^*) > M_{Y'}(X^*)|Y^*, M_{Y^*}(X^*), X^*]. \tag{9}$$

The distribution of U^* will depend on π, $\{F_y\}_{y\in\mathcal{S}}$ and $\{\nu_y\}_{y\in\mathcal{S}}$, and generally cannot be written in a closed form. However, this distribution is central to our analysis–indeed, we will see that the function D appearing in theorem 3 is defined as the cumulative distribution function of U^*.

The special case of $k = 2$ shows the relation between the distribution of U^* and the average generalization accuracy, AGA_2. In the two-class case, the average generalization accuracy is the probability that a random correct label score function gives a larger value than a random distractor:

$$\mathrm{AGA}_2 = \Pr[M_{Y^*}(X^*) > M_{Y'}(X^*)].$$

where Y^* is the correct label, and Y' is a random incorrect label. If we condition on Y^*, M_{Y^*} and X^*, we get

$$\mathrm{AGA}_2 = \mathbf{E}[\Pr[M_{Y^*}(X^*) > M_{Y'}(X^*)|Y^*, M_{Y^*}, X^*]].$$

Here, the conditional probability inside the expectation is the correct-label favorability. Therefore,

$$\mathrm{AGA}_2 = \mathbf{E}[U^*] = \int D(u)du,$$

where $D(u)$ is the cumulative distribution function of U^*, $D(u) = \Pr[U^* \le u]$. Theorem 3 extends this to general k; we now give the proof.

Proof Without loss of generality, suppose that the true label is Y^* and the incorrect labels are $Y^{(1)}, \ldots, Y^{(k-1)}$. We have

$$\mathrm{AGA}_k = \Pr[M_{Y^*}(X^*) > \max_{i=1}^{k-1} M_{Y^{(i)}}(X^*)] = \Pr[U^* > \max_{i=1}^{k-1} U_{X^*}(M_{Y^{(i)}})],$$

recalling that $U^* = U_{X^*}(M_{Y^*})$. Now, if we condition on $X^* = x^*$, $Y^* = y^*$ and $M_{Y^*} = m_{y^*}$, then the random variable U^* becomes fixed, with value

$$u^* = U_{x^*}(m_{y^*}).$$

Therefore,

$$\begin{aligned}\mathrm{AGA}_k &= \mathbf{E}[\Pr[U^* > \max_{i=1}^{k-1} U_{X^*}(M_{Y^{(i)}})|X^* = x^*, Y^* = y^*, M_{Y^*} = m_{y^*}]] \\ &= \mathbf{E}[\Pr[U^* > \max_{i=1}^{k-1} U_{X^*}(M_{Y^{(i)}})|X^* = x^*, U^* = u^*]].\end{aligned}$$

Now define $U_{max,k-1} = \max_{i=1}^{k-1} U_{X^*}(M_{Y^{(i)}})$. Since by Lemma 4, $U_{X^*}(M_{Y^{(i)}})$ are i.i.d. uniform conditional on $X^* = x^*$, we know that

$$U_{max,k-1}|X^* = x^* \sim \mathrm{Beta}(k-1, 1). \tag{10}$$

Furthermore, $U_{max,k-1}$ is independent of U^* conditional on X^*. Therefore, the conditional probability can be computed as

$$\Pr[U^* > U_{max,k-1}|X^* = x^*, U^* = u^*] = \int_0^{u^*} (k-1)u^{k-2}du.$$

Consequently,

$$\mathrm{AGA}_k = \mathbf{E}[\Pr[U^* > \max_{i=1}^{k-1} U_{X^*}(M_{Y^{(i)}})|X^* = x^*, U^* = u^*]] \tag{11}$$

$$= \mathbf{E}[\int_0^{U^*} (k-1)u^{k-2}du|U^* = u^*] \tag{12}$$

$$= \mathbf{E}[\int_0^1 I\{u \le U^*\}(k-1)u^{k-2}du] \tag{13}$$

$$= (k-1)\int_0^1 \Pr[u \le U^*]u^{k-2}du \tag{14}$$

$$= 1 - (k-1)\int_0^1 \Pr[u \ge U^*]u^{k-2}du. \tag{15}$$

By defining $D(u)$ as the cumulative distribution function of U^* on $[0, 1]$,

$$D(u) = \Pr[U_{X^*}(M_{Y^*}) \le u], \tag{16}$$

and substituting this definition into (15), we obtain the identity (5). ■

Theorem 3 expresses the average accuracy as a weighted integral of the function $D(u)$. Essentially, this theoretical result allows us to reduce the problem of estimating AGA_k to one of estimating $D(u)$. But how shall we estimate $D(u)$ from data? We propose using non-parametric regression for this purpose in Section 3.3.

3.2. Favorability and Average Accuracy for the Toy Example

Recall that for the toy example from Section 2.4, the score function M_y was a non-random function of y that measures the distance between x and ρy

$$M_y(x^*) = \log(p(x^*|y)) = -\frac{(x^* - \rho y)^2}{2(1-\rho^2)}.$$

For this model, the favorability function $U_{x^*}(m_y)$ compares the distance between x^* and ρy to the distance between x^* and $\rho Y'$ for a randomly chosen distractor $Y' \sim N(0,1)$:

$$\begin{aligned} U_{x^*}(m_y) &= \Pr[|\rho y - x^*| < |\rho Y' - x^*|] \\ &= \Phi\left(\frac{x^* + |\rho y - x^*|}{\rho}\right) - \Phi\left(\frac{x^* - |\rho y - x^*|}{\rho}\right), \end{aligned}$$

where Φ is the standard normal cumulative distribution function. Figure 5(a) illustrates the level sets of the function $U_{x^*}(m_y)$. The highest values of $U_{x^*}(m_y)$ are near the line $x^* = \rho y$ corresponding to the conditional mean of $X|Y$, and as one moves farther from the line, $U_{x^*}(m_y)$ decays. Note, however, that large values of x^* and y (with the same sign) result in larger values of $U_{x^*}(m_y)$ since it becomes unlikely for $Y' \sim N(0,1)$ to exceed $Y = y$.

Using the formula above, we can calculate the correct-label favorability $U^* = U_{X^*}(M_{Y^*})$ and its cumulative distribution function $D(u)$. The function D is illustrated in Figure 5(b) for the current example with $\rho = 0.7$. The red curve in Figure 4 was computed using the formula

$$\mathrm{AGA}_k = 1 - (k-1)\int D(u)u^{k-2}du.$$

It is illuminating to consider how the average accuracy curves and the $D(u)$ functions vary as we change the parameter ρ. Higher correlations ρ lead to higher accuracy, as seen in Figure 6(a), where the accuracy curves are shifted upward as ρ increases from 0.3 to 0.9. The favorability $U_{x^*}(m_y)$ tends to be higher on average as well, which leads to lower values of the cumulative distribution function–as we see in Figure 6(b), where the function $D(u)$ decreases as ρ increases, and therefore accuracy increases.

3.3. Estimation

Next, we discuss how to use data from smaller classification tasks to extrapolate average accuracy. We are seeking an unbiased estimator $\widehat{\mathrm{AGA}_k}$ such that

$$\mathbf{E}[\widehat{\mathrm{AGA}_k}] = \mathrm{AGA}_k.$$

Assume that we have data from a k_1-class random classification task, and would like to estimate the average accuracy AGA_{k_2} for $k_2 > k_1$ classes. Our estimation method will use the k-class average test accuracies, $\mathrm{ATA}_2, ..., \mathrm{ATA}_{k_1}$ (see Eq 4), for its inputs.

The key to understanding the behavior of the average accuracy AGA_k is the function D. We adopt a linear model

$$D(u) = \sum_{\ell=1}^{m} \beta_\ell h_\ell(u), \tag{17}$$

where $h_\ell(u)$ are known basis functions, and β_ℓ are the linear coefficients to be estimated. The linearity assumption (17) means that linear regression can be used to estimate the average accuracy curve. This the the idea behind our proposed method ClassExReg, meaning *Classification Extrapolation using Regression.*

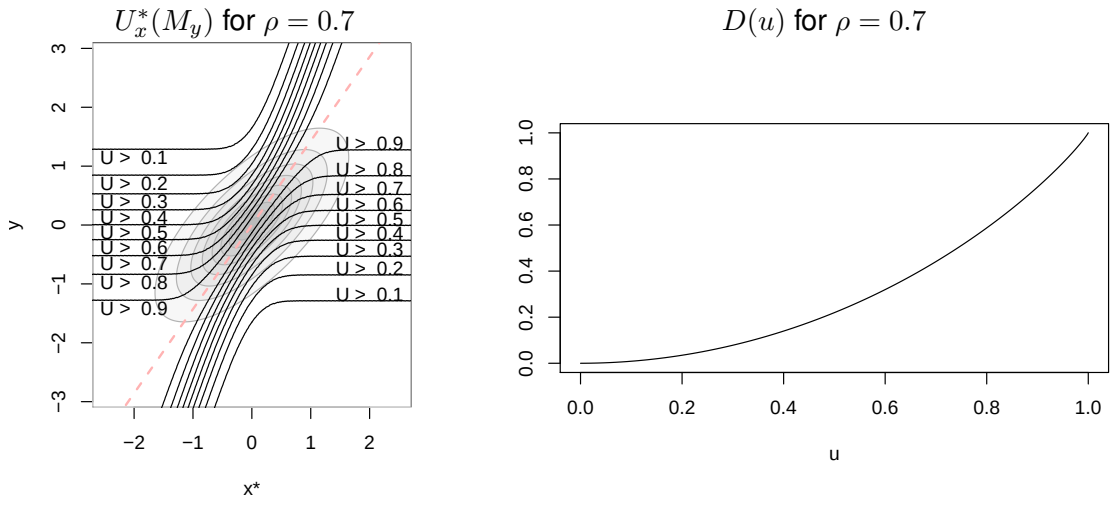

Figure 5: **Favorability for toy example:** *Left:* The level curves of the function $U_{x^*}(M_y)$ in the bivariate normal model with $\rho = 0.7$. *Right:* The function $D(u)$ gives the cumulative distribution function of the random variable $U_{X^*}(M_Y)$.

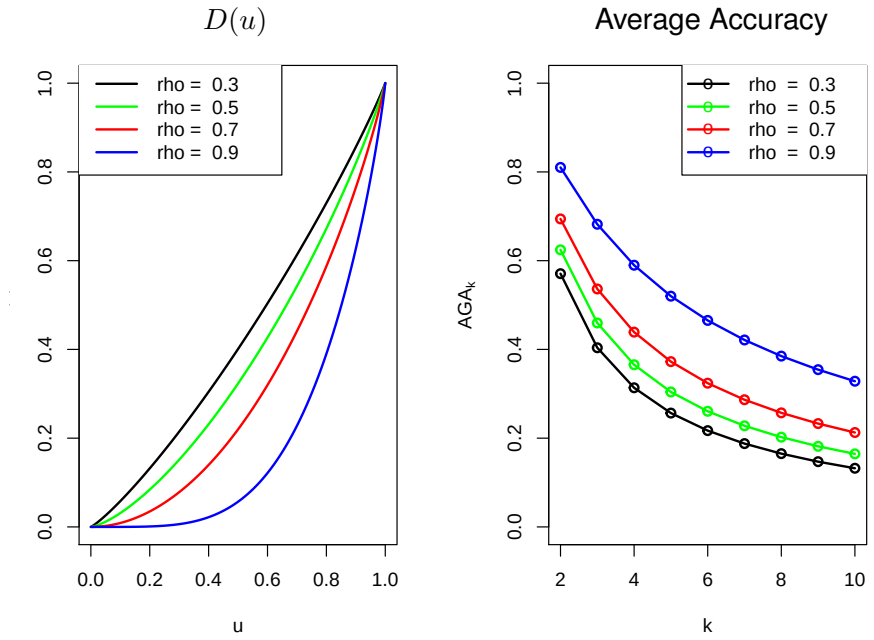

Figure 6: **Average accuracy with different ρ's:** *Left:* The average accuracy AGA_k. *Right:* $D(u)$ function for the bivariate normal model with $\rho \in \{0.3, 0.5, 0.7, 0.9\}$.

Conveniently, AGA_k can also be expressed in terms of the β_ℓ coefficients. If we plug in the assumed linear model (17) into the identity (5), then we get

$$1 - \mathrm{AGA}_k = (k-1) \int D(u) u^{k-2} du \tag{18}$$

$$= (k-1) \int_0^1 \sum_{\ell=1}^{m} \beta_\ell h_\ell(u) u^{k-2} du \tag{19}$$

$$= \sum_{\ell=1}^{m} \beta_\ell H_{\ell,k}, \tag{20}$$

where

$$H_{\ell,k} = (k-1) \int_0^1 h_\ell(u) u^{k-2} du. \tag{21}$$

The constants $H_{\ell,k}$ are moments of the basis function h_ℓ. Note that $H_{\ell,k}$ can be precomputed numerically for any $k \geq 2$.

Now, since the test accuracies ATA_k are unbiased estimates of AGA_k, this implies that the regression estimate

$$\hat{\beta} = \mathrm{argmin}_\beta \sum_{k=2}^{k_1} \left((1 - \mathrm{ATA}_k) - \sum_{\ell=1}^{m} \beta_\ell H_{\ell,k} \right)^2,$$

is unbiased for β. The estimate of AGA_{k_2} is similarly obtained from (20), via

$$\widehat{\mathrm{AGA}_{k_2}} = 1 - \sum_{\ell=1}^{m} \hat{\beta}_\ell H_{\ell,k_2}. \tag{22}$$

3.4. Model Selection

Accurate extrapolation using ClassExReg depends on a good fit between the linear model (17) and the true discriminability function $D(u)$. However, since the function $D(u)$ depends on the unknown joint distribution of the data, it makes sense to let the data help us choose a good basis $\{h_u\}$ from a set of candidate bases.

Let $B_1, \ldots, B_s$ be a set of candidate bases, with $B_i = \{h_u^{(i)}\}_{u=1}^{m_i}$. Ideally, we would like our model selection procedure to choose the B_i that obtains the best root-mean-squared error (RMSE) on the extrapolation from k_1 to k_2 classes. As an approximation, we estimate the RMSE of extrapolation from $\frac{k_1}{2}$ source classes to k_1 target classes, by means of the "bootstrap principle." This amounts to a resampling-based model selection approach, where we perform extrapolations from $k_0 = \lfloor \frac{k_1}{2} \rfloor$ classes to k_1 classes, and evaluate methods based on how closely the predicted $\widehat{\mathrm{AGA}}_{k_1}$ matches the test accuracy ATA_{k_1}. To elaborate, our model selection procedure is as follows.

1. For $\ell = 1, \ldots, L$ resampling steps:
   (a) Subsample $\mathcal{S}_{k_0}^{(\ell)}$ from $\mathcal{S}_{k_1}$ uniformly with replacement.
   (b) Compute average test accuracies $\mathrm{ATA}_2^{(\ell)}, \ldots, \mathrm{ATA}_{k_0}^{(\ell)}$ from the subsample $\mathcal{S}_{k_0}^{(\ell)}$.

(c) For each candidate basis B_i, with $i = 1, \ldots, s$:

i. Compute $\hat{\beta}^{(i,\ell)}$ by solving the least-squares problem

$$\hat{\beta}^{(i,\ell)} = \text{argmin}_\beta \sum_{k=2}^{k_0} \left((1 - \text{ATA}_k^{(\ell)}) - \sum_{j=1}^{m_i} \beta_j H_{j,k}^{(i)} \right)^2 .$$

ii. Estimate $\widehat{\text{AGA}}_{k_1}^{(i,\ell)}$ by

$$\widehat{\text{AGA}}_{k_1}^{(i,\ell)} = \sum_{\ell=1}^{m_i} \hat{\beta}_j^{(i,\ell)} H_{j,k_1}^{(i)}.$$

2. Select the basis B_{i^*} by

$$i^* = \text{argmin}_{i=1}^{s} \sum_{\ell=1}^{L} (\widehat{\text{AGA}}_{k_1}^{(i,\ell)} - \text{ATA}_{k_1})^2.$$

3. Use the basis B_{i^*} to extrapolate from k_1 classes (the full data) to k_2 classes.

3.5. The Kay KDE-based estimator

In their paper,[3] Kay et al. (2008) proposed a method for extrapolating classification accuracy to a larger number of classes. The method depends on repeated kernel-density estimation (KDE) steps. Because the method is only briefly motivated in the original text, we present it in our notation.

The idea of the method is to estimate separately for each example $x_\ell^{(i)}$ associated with class $y^{(i)}$ the probability of outscoring a random competitor:

$$\text{Acc}_2(x_\ell^{(i)}; m) := \Pr[m_\ell^{(i,i)} > m_Y(x_\ell^{(i)})],$$

recalling that we defined $m_\ell^{(i,j)} = m_{y^{(j)}}(x_\ell^{(i)})$. For a given example, accurate classification against $k-1$ independent (random) distractor classes is equivalent to $k-1$ independent accurate classifications of a single random competitor. Therefore,

$$\text{Acc}_k(x_\ell^{(i)}; m_{y^{(i)}}) := \Pr[m_\ell^{(i,i)} > \max_{j \neq i} m_\ell^{(i,j)}] = \text{Acc}_2(x_\ell^{(i)}; m_{y^{(i)}})^{k-1}.$$

Given estimated accuracy values $a_\ell^{(i)} = \widehat{\text{Acc}}_2(x_\ell^{(i)})$, $\ell = 1, \ldots, r$, $i = 1, ..., k_1$, we can average the $k-1$ powers:

$$\widehat{\text{AGA}}_k = \frac{1}{rk_1} \sum_{i=1}^{k_1} \sum_{\ell=1}^{r} (1 - (1 - a_\ell^{(i)})^{k-1})$$

Note that if we have noisy but unbiased estimates of $\text{Acc}_2(x_\ell^{(i)}; m_{y^{(i)}})$, then the estimates for $\text{Acc}_k(x_\ell^{(i)}; m_{y^{(i)}})$ and $\widehat{\text{AGA}}_K$ will be upward biased because $\mathbf{E}[X^K] \geq \mathbf{E}[X]^K$.

Accuracy for each example $\text{Acc}_2(x_\ell^{(i)})$ is estimated in two steps:

3. The KDE extrapolation method is described in page 29 of supplement to Kay et al. (2008). While the method is only described for a one-nearest neighbor classifier and for the setting where there is at most one test observation per class, we have taken the liberty of extending it to a generic multi-class classification problem.

1. The density of the wrong-class scores is estimated by smoothing the observed scores with a kernel function $K(\cdot,\cdot)$ and bandwidth h

$$\hat{f}_\ell^{(i)}(m) = \frac{1}{k_1 - 1}\sum_{j\neq i} K_h(m_\ell^{(i,j)}, m).$$

2. The density $\hat{f}_\ell^{(i)}(m)$ is integrated below the observed true value $m_\ell^{(i,i)}$:

$$a_\ell^{(i)} = \widehat{\mathrm{Acc}}_2(x_\ell^{(i)}) = \int_{-\infty}^{m_\ell^{(i,i)}} \hat{f}_\ell^{(i)}(m)dm.$$

The smoothed density usually over-estimates the size of the right-tail of wrong class distribution compared to the observed proportion of errors, biasing downward the accuracy of each individual example.

Briefly, let us point out several key differences between our regression method and Kay's KDE method:

i. The KDE method balances two biases: an upward bias in exponentiating the estimated accuracy, and a downward bias in smoothing the wrong-class densities. The upward bias occurs because even if $\widehat{\mathrm{Acc}}_2(x_\ell^{(i)})$ is unbiased, $\widehat{\mathrm{Acc}}_2(x_\ell^{(i)})^k$ will *not* be unbiased for $\mathrm{Acc}_2(x_\ell^{(i)})^k$, and will typically be larger. The bias becomes more prominent for larger k, but decreases as the true accuracy approaches 1. The result of the KDE method therefore depends non-trivially on the choice of smoothing bandwidth used in the density estimation step. (Without smoothing, however, any example that was correctly estimated in the smaller set would have $\widehat{\mathrm{Acc}}_K = 1$). The method relies on smoothing of each class to generate the tail density that exceeds $m_\ell^{(i,i)}$, and therefore it is highly dependent on the choice of kernel bandwidth.

ii. The KDE method estimates the accuracy separately for every class. When the source-set size k is small, this might lead to less stable estimation for each class and therefore a larger bias after extrapolating. The regression estimator, on the other hand, estimates the average accuracy pooling together information across classes. This might lead to higher variance.

iii. The regression method does not look at the scores directly, only at the rankings. It is therefore blind to monotone transformations on the score functions. The KDE method, on the other hand, is sensitive to the distribution of observed scores.

4. Simulation Study

We ran simulations to check how the proposed extrapolation method, ClassExReg, performs in different settings. The results are displayed in Figure 7. We varied the number of classes k_1 in the source data set, the difficulty of classification, and the basis functions. We generated data according to a mixture of isotropic multivariate Gaussian distributions: labels Y were sampled from $Y \sim N(0, I_{10})$, and the examples for each label sampled from $X|Y \sim N(Y, \sigma^2 I_{10})$. The noise-level parameter σ determines the difficulty of classification.

Similarly to the real-data example, we consider a 1-nearest neighbor classifier, which is given a single training instance per class.

For the estimation, we use the model selection procedure described in Section 3.4 to select the parameter h of the "radial basis"

$$h_\ell(u) = \Phi\left(\frac{\Phi^{-1}(u) - t_\ell}{h}\right).$$

where t_ℓ are a set of regularly spaced knots which are determined by h and the problem parameters. Additionally, we add a constant element to the basis, equivalent to adding an intercept to the linear model (17).

The rationale behind the radial basis is to model the density of $\Phi^{-1}(U^*)$ as a mixture of Gaussian kernels with variance h^2. To control overfitting, the knots are separated by at least a distance of $h/2$, and the largest knots have absolute value $\Phi^{-1}(1 - \frac{1}{rk_1^2})$. The size of the maximum knot is set this way since rk_1^2 is the number of ranks that are calculated and used by our method. Therefore, we do not expect the training data to contain enough information to allow our method to distinguish between more than rk_1^2 possible accuracies, and hence we set the maximum knot to prevent the inclusion of a basis element that has on average a higher mean value than $u = 1 - \frac{1}{rk_1^2}$. However, in simulations we find that the performance of the basis depends only weakly on the exact positioning and maximum size of the knots, as long as sufficiently large knots are included. As is the case throughout non-parametric statistics, the bandwidth h is the most crucial parameter. In the simulation, we use a grid $h = \{0.1, 0.2, \ldots, 1\}$ for bandwidth selection.

Meanwhile, for the KDE method, we used a Gaussian kernel, with the bandwidth chosen via pseudolikelihood cross-validation (Cao et al., 1994), as recommended by Kay et al. (2008). Specifically, we used the two methods for cross-validated KDE estimation provided in the `stats` package in the `R` statistical computing environment: biased cross-validation and unbiased cross-validation (Scott, 1992).

4.1. Simulation Results

We see in Figure 7 that ClassExReg and the KDE methods with unbiased and biased cross-validation (KDE-UCV, KDE-BCV) perform comparably in the Gaussian simulations. We studied how the difficulty of extrapolation relates to both the absolute size of the number of classes and the extrapolation factor $\frac{k_2}{k_1}$. Our simulation has two settings for $k_1 = \{500, 5000\}$, and within each setting we have extrapolations to 2 times, 4 times, 10 times, and 20 times the number of classes.

Within each problem setting defined by the number of source and target classes (k_1, k_2), we use the maximum RMSE across all signal-to-noise settings to quantify the overall performance of the method, as displayed in Table 1.

The results also indicate that more accurate extrapolation appears to be possible for smaller extrapolation ratios $\frac{k_2}{k_1}$ and larger k_1. ClassExReg improves in worst-case RMSE when moving from $k_1 = 500$ to $k_1 = 5000$ while keeping the extrapolation factor fixed, most dramatically in the case $\frac{k_2}{k_1} = 2$ when it improves from a maximum RMSE of 0.032 ± 0.001 ($k_1 = 500$) to 0.009 ± 0.000 ($k_1 = 5000$), which is 3.5-fold reduction in worst-case RMSE,

k_1	k_2	ClassExReg	KDE-BCV	KDE-UCV
500	1000	**0.032** (0.001)	0.090 (0.001)	0.067 (0.001)
500	2000	**0.044** (0.002)	0.088 (0.001)	0.059 (0.001)
500	5000	0.073 (0.004)	0.079 (0.001)	**0.051** (0.001)
500	10000	0.098 (0.004)	0.076 (0.001)	**0.045** (0.001)
5000	10000	**0.009** (0.000)	0.038 (0.000)	0.028 (0.000)
5000	20000	**0.015** (0.001)	0.028 (0.000)	0.019 (0.000)
5000	50000	**0.032** (0.002)	0.035 (0.000)	0.053 (0.000)
5000	100000	**0.054** (0.003)	0.065 (0.000)	0.086 (0.000)

Table 1: Maximum RMSE (se) across all signal-to-noise-levels in predicting TA_{k_2} from k_1 classes in multivariate Gaussian simulation. Standard errors were computed by nesting the maximum operation within the bootstrap, to properly account for the variance of a maximum of estimated means.

but also benefiting from at least a 1.8-fold reduction in RMSE when going from the smaller problem to the larger problem in the other three cases.

The kernel-density method produces comparable results, but is seen to depend strongly on the choice of bandwidth selection: KDE-UCV and KDE-BCV show very different performance profiles, although they differ only in the method used to choose the bandwidth. This matches our analysis in Section 3.5 (item i), where we noted the sensitivity of the tail densities to the bandwidth. Also, the KDE methods show significant estimation bias, as can be seen from Figure 8. As we discussed in 3.5 (item i), this is due to the fact that the KDE method ignores the bias introduced by exponentiation. Meanwhile, ClassExReg avoids this source of bias by estimating the $(k-1)$st moment of $D(u)$ directly. As we see in Figure 8, correcting for the bias of exponentiation helps greatly to reduce the overall bias. Indeed, while ClassExReg shows comparable bias for the 500 to 10000 extrapolation, the bias is very well-controlled in all of the $k_1 = 5000$ extrapolations.

5. Experimental Evaluation

We demonstrate the extrapolation of average accuracy in two data examples: (i) predicting the accuracy of a face recognition on a large set of labels from the system's accuracy on a smaller subset, and (ii) extrapolating the performance of various classifiers on an optical character recognition (OCR) problem in the Telugu script, which has over 400 glyphs.

The face-recognition example takes data from the "Labeled Faces in the Wild" data set (Huang et al. (2007)), where we selected the 1672 individuals with at least 2 face photos. We form a data set consisting of photo-label pairs $(x_j^{(i)}, y^{(i)})$ for $i = 1, \ldots, 1672$ and $j = 1, 2$ by randomly selecting 2 face photos for each individual. We used the OpenFace (Amos et al. (2016)) embedding for feature extraction.[4] In order to identify a new photo x^*, we obtain the feature vector $g(x^*)$ from the OpenFace network, and guess the label $\hat{y}$ with the

4. For each photo x, a 128-dimensional feature vector $g(x)$ is obtained as follows. The computer vision library DLLib is used to detect landmarks in x, and to apply a nonlinear transformation to align x to a template. The aligned photograph is then downsampled to a 96×96 image. The downsampled image

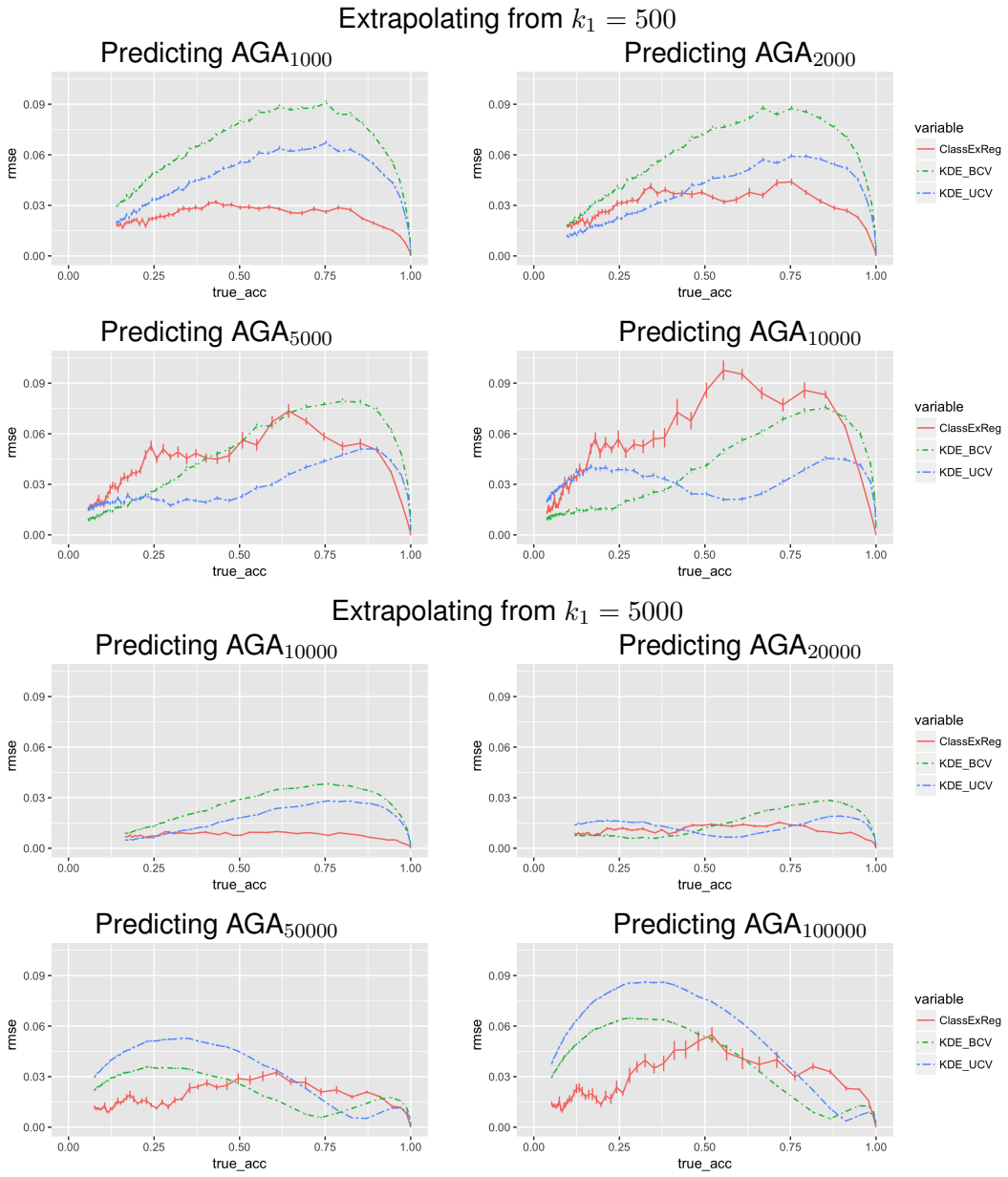

Figure 7: **Simulation results (RMSE):** Simulation study consisting of multivariate Gaussian Y with nearest neighbor classifier. Prediction RMSE vs true k_2-class accuracy for ClassExReg with radial basis (ClassExReg), KDE-based methods with biased cross-validation (KDE_BCV) and unbiased cross-validation (KDE_UCV).

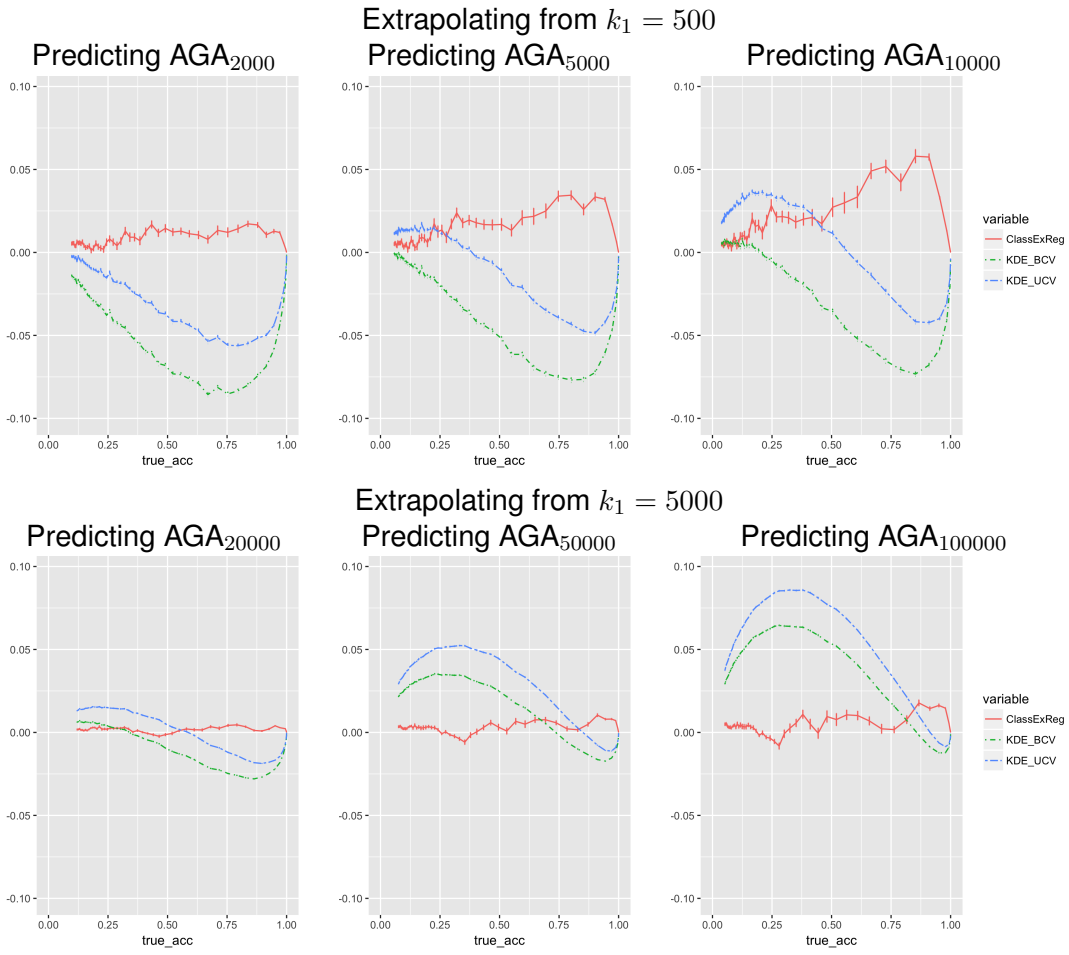

Figure 8: **Simulation results (biases):** Simulation study consisting of multivariate Gaussian Y with nearest neighbor classifier. Bias (mean predicted minus true accuracy) vs true k_2-class accuracy for ClassExReg with radial basis (ClassExReg), KDE-based methods with biased cross-validation (KDE_BCV) and unbiased cross-validation (KDE_UCV).

Label	Training	Test
$y^{(1)}$=Amelia	$x_0^{(1)}$ =	$x_1^{(1)}$ =
$y^{(2)}$=Jean-Pierre	$x_0^{(2)}$ =	$x_1^{(2)}$ =
$y^{(3)}$=Liza	$x_0^{(3)}$ =	$x_1^{(3)}$ =
$y^{(4)}$=Patricia	$x_0^{(4)}$ =	$x_1^{(4)}$ =

Figure 9: **Face recognition setup (top):** Examples of labels and features from the *Labeled Faces in the Wild* data set. **Telugu OCR (bottom)**: exemplars from six of the glyph classes, along with intermediate features and final transformations from the deep convolutional network.

minimal Euclidean distance between $g(y^{(i)})$ and $g(x^*)$, which implies a score function

$$M_{y^{(i)}}(x^*) = -||g(x_1^{(i)}) - g(x^*)||^2.$$

In this way, we can compute the test accuracy on all 1672 classes, TA_{1672}, but we also subsample $k_1 = \{100, 200, 400\}$ classes in order to extrapolate from k_1 to 1672 classes.

In the Telugu optical character recognition example (Achanta and Hastie (2015)), we consider the use of three different classifiers: logistic regression, linear support-vector machine (SVM), and a deep convolutional neural network.[5] The full data consists of 400 classes with 50 training and 50 test observations for each class. We create a nested hierarchy of subsampled data sets consisting of (i) a subset of 100 classes uniformly sampled without replacement from the 400 classes, and (ii) a subset consisting of 20 classes uniformly sampled without replacement from the size-100 subsample. We therefore study three different prediction extrapolation problems:

1. Predicting the accuracy on $k_2 = 100$ classes from $k_1 = 20$ classes, comparing the predicted accuracy to the test accuracy of the classifier on the 100-class subsample as ground truth.

is fed into a pre-trained deep convolutional neural network to obtain the 128-dimensional feature vector $g(x)$. More details are found in Amos et al. (2016).

5. The network architecture is as follows: `48x48-4C3-MP2-6C3-8C3-MP2-32C3-50C3-MP2-200C3-SM`.

k_1	ClassExReg	KDE-BCV	KDE-UCV
100	0.113 (0.002)	**0.053** (0.001)	0.082 (0.001)
200	0.058 (0.002)	**0.037** (0.001)	0.057 (0.001)
400	0.050 (0.001)	**0.024** (0.001)	0.035 (0.001)

Table 2: **Face-recognition extrapolation RMSEs**: RMSE (se) on predicting TA_{1672} from k_1 classes

2. Same as (1), but setting $k_2 = 400$ and $k_1 = 20$, and using the full data set for the ground truth.

3. Same as (2), but setting $k_2 = 400$ and $k_1 = 100$.

Note that unlike in the case of the face recognition example, here the assumption of marginal classification is satisfied for none of the classifiers. We compare the result of our model to the ground truth obtained by using the full data set.

5.1. Results

The extrapolation results for the face recognition problem can be seen in Figure 10, which plots the extrapolated accuracy curves for each method for 100 different subsamples of size k_1. As can be seen, for all three methods, the variances decrease rapidly as k_1 increases.

The root-mean-square errors at $k_2 = 1672$ can be seen in Table 2. KDE-BCV achieves the best extrapolation for all three cases $k_1 = \{100, 200, 400\}$ with KDE-UCV consistently achieving second place. These results differ from the ranking of the RMSEs for the analagous simulation when predicting $k_2 = 2000$ from $k_1 = 500$ for accuracies around 0.45: in the first row and second column of Figure 7, where the true accuracy is 0.43 (from setting $\sigma^2 = 0.2$), the lowest RMSE belongs to KDE-UCV (RMSE=0.0361 ± 0.001), followed closely by ClassExReg (RMSE=0.0372 ± 0.002), and KDE-BCV (RMSE=0.0635 ± 0.001) having the highest RMSE. These discrepancies could be explained by differences between the data distributions between the simulation and the face recognition example, and also by the fact that we only have access to the $k_2 = 1672$-class ground truth for the real data example.

The results for Telugu OCR classification are displayed in Table 3. If we rank the three extrapolation methods in terms of distance to the ground truth accuracy, we see a consistent pattern of rankings between the 20-to-100 extrapolation and the 100-to-400 extrapolation. As we remarked in the simulation, the difficulty of extrapolation appears to be primarily sensitive to the extrapolation ratio $\frac{k_2}{k_1}$, which are similar (5 versus 4) in the 20-to-100 and 100-to-400 problems. In both settings, ClassExReg comes closest to the ground truth for the Deep CNN and the SVM, but KDE-BCV comes closest to ground truth for the Logistic regression. However, even for logistic regression, ClassExReg does better or comparably to KDE-UCV.

In the 20-to-400 extrapolation, which has the highest extrapolation ratio ($\frac{k_2}{k_1} = 20$), none of the three extrapolation methods performs consistently well for all three classifiers. It could be the case that the variability is a dominating effect given the small training

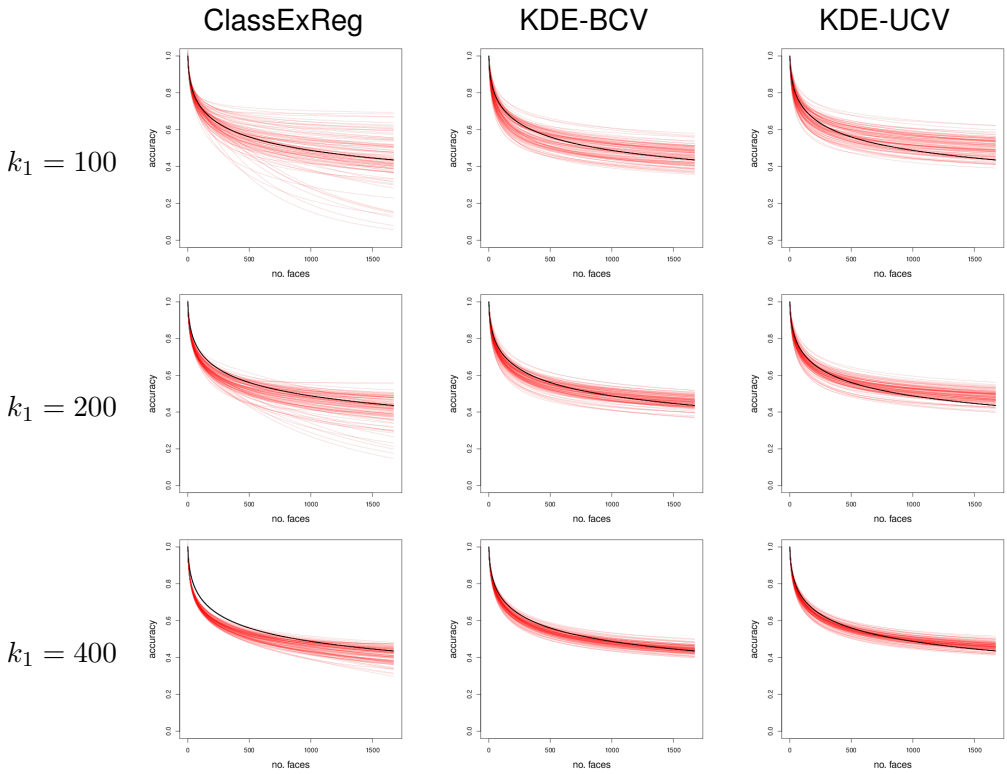

Figure 10: **Predicted accuracy curves for face-recognition example**: The plots show predicted accuracies. Each red curve represents the predicted accuracies using a single subsample of size k_1. The black curve shows the average test accuracy obtained from the full data set.

set, making it difficult to compare extrapolation methods using the 20-to-400 extrapolation task.

Unlike in the face recognition example, we did not resample training classes here, because that would require retraining all of the classifiers–which would be prohibitively time-consuming for the Deep CNN. Thus, we cannot comment on the robustness of the comparisons from this example, though it is likely that we would obtain different rankings under a new resampling of the training classes.

These empirical results indicate that in comparison to the KDE methods of Kay et al., ClassExReg has lower bias and better performance at small k (up to 500 classes), while the KDE methods start to achieve comparable results to ClassExReg when k is around 5,000 or more classes. This matches the theoretical intuition we developed in Section 3.5 (item ii): since the Kay et al. method works by estimating each the favorability of each example separately, that it requires more data (meaning more classes in the training set) to achieve robust estimation.

k_1	k_2	Classifier	True	ClassExReg	KDE-BCV	KDE-UCV
20	100	Deep CNN	0.9908	**0.9905**	0.7138	0.6507
		Logistic	0.8490	0.8980	**0.8414**	0.8161
		SVM	0.7582	**0.8192**	0.6544	0.5771
20	400	Deep CNN	0.9860	**0.9614**	0.4903	0.3863
		Logistic	0.7107	0.8824	0.7467	**0.7015**
		SVM	0.5452	0.6725	**0.5163**	0.4070
100	400	Deep CNN	0.9860	**0.9837**	0.8910	0.8625
		Logistic	0.7107	0.7214	**0.7089**	0.6776
		SVM	0.5452	**0.5969**	0.4369	0.3528

Table 3: **Telugu OCR extrapolated accuracies**: Extrapolating from k_1 to k_2 classes in Telugu OCR for three different classifiers: logistic regression, support vector machine, and deep convolutional network

6. Discussion

In this work, we suggest treating the class set in a classification task as random, in order to extrapolate classification performance on a small task to the expected performance on a larger unobserved task. We show that average generalized accuracy decreases with increased label set size like the $(k-1)$th moment of a distribution function. Furthermore, we introduce an algorithm for estimating this underlying distribution, that allows efficient computation of higher order moments. We additionally implement a kernel-density estimation based extrapolation, and discuss different regimes were the methods are useful. Code for the methods and the simulations can be found in `https://github.com/snarles/ClassEx`.

There are many choices and simplifying assumptions used in the description of the method. Here we discuss these decisions and map some alternative models or strategies for future work.

Two important practical aspects of real-world problems not currently handled by our analysis are (i) non-uniform prior distributions on the labels, and (ii) cost functions other than zero-one loss. In fact, a theory for arbitrary cost functions can double as a theory for non-uniform priors, because the risk incurred under non-uniform priors is equivalent to the risk incurred under a uniform prior but with a weighted cost function. Hence, we address both (i) and (ii) in forthcoming work that shows how performance extrapolation is possible under arbitrary cost functions.

Since our analysis is currently restricted to i.i.d. sampling of classes, one direction for future work is to generalize the sampling mechanism, such as to cluster sampling. More broadly, the assumption that the labels in $\mathcal{S}_k$ are a random sample from a homogeneous distribution π may be inappropriate. Many natural classification problems arise from hierarchically partitioning a space of instances into a set of labels. Therefore, rather than modeling $\mathcal{S}_k$ as a random sample, it may be more suitable to model it as a random hierarchical partition of $\mathcal{Y}$, such as one arising from an optional Pólya tree process (Wong and Ma, 2010). Finally, note that we assume no knowledge about the new class-set except for its size. Better accuracy might be achieved if some partial information is known.

A third direction of exploration is to impose additional modeling assumptions for specific problems. ClassExReg adopts a non-parametric model of the discriminability function $D(u)$, in the sense that $D(u)$ was defined via a spline expansion. However, an alternative approach is to assume a parametric family for $D(u)$ defined by a small number of parameters. In forthcoming work, we show that under certain limiting conditions, $D(u)$ is well-described by a two-parameter family. This substantially increases the efficiency of estimation in cases where the limiting conditions are well-approximated.

Acknowledgments

We thank Jonathan Taylor, Trevor Hastie, John Duchi, Steve Mussmann, Qingyun Sun, Robert Tibshirani, Patrick McClure, Francisco Pereira, and Gal Elidan for useful discussion. CZ is supported by an NSF graduate research fellowship, and would also like to thank the European Research Council under the ERC grant agreement n°[PSARPS-294519] for travel support. We would also like thank the anonymous reviewers for their comments, which improved the readability of the paper.

References

Felix Abramovich and Marianna Pensky. Feature selection and classification of high-dimensional normal vectors with possibly large number of classes. *arXiv preprint arXiv:1506.01567*, 2015.

Rakesh Achanta and Trevor Hastie. Telugu OCR framework using deep learning. *arXiv preprint arXiv:1509.05962*, 2015.

Brandon Amos, Bartosz Ludwiczuk, and Mahadev Satyanarayanan. Openface: A general-purpose face recognition library with mobile applications. Technical report, CMU-CS-16-118, CMU School of Computer Science, 2016.

Ricardo Cao, Antonio Cuevas, and Wensceslao González Manteiga. A comparative study of several smoothing methods in density estimation. *Computational Statistics & Data Analysis*, 17(2):153–176, 1994.

Koby Crammer and Yoram Singer. On the algorithmic implementation of multiclass kernel-based vector machines. *Journal of Machine Learning Research*, 2(Dec):265–292, 2001.

Justin Davis, Marianna Pensky, and William Crampton. Bayesian feature selection for classification with possibly large number of classes. *Journal of Statistical Planning and Inference*, 141(9):3256–3266, 2011.

Jia Deng, Alexander C Berg, Kai Li, and Li Fei-Fei. What does classifying more than 10,000 image categories tell us? In *European conference on computer vision*, pages 71–84. Springer, 2010.

Jeff Donahue, Yangqing Jia, Oriol Vinyals, Judy Hoffman, Ning Zhang, Eric Tzeng, and Trevor Darrell. Decaf: A deep convolutional activation feature for generic visual recognition. In *International conference on machine learning*, pages 647–655, 2014.

Pinar Duygulu, Kobus Barnard, Joao FG de Freitas, and David A Forsyth. Object recognition as machine translation: Learning a lexicon for a fixed image vocabulary. In *European conference on computer vision*, pages 97–112. Springer, 2002.

Gregory Griffin, Alex Holub, and Pietro Perona. Caltech-256 object category dataset. 2007.

Maya R Gupta, Samy Bengio, and Jason Weston. Training highly multiclass classifiers. *Journal of Machine Learning Research*, 15(1):1461–1492, 2014.

Gary B. Huang, Manu Ramesh, Tamara Berg, and Erik Learned-Miller. Labeled faces in the wild: A database for studying face recognition in unconstrained environments. Technical Report 07-49, University of Massachusetts, Amherst, October 2007.

Kendrick N Kay, Thomas Naselaris, Ryan J Prenger, and Jack L Gallant. Identifying natural images from human brain activity. *Nature*, 452(March):352–355, 2008.

Yoonkyung Lee, Yi Lin, and Grace Wahba. Multicategory support vector machines: Theory and application to the classification of microarray data and satellite radiance data. *Journal of the American Statistical Association*, 99(465):67–81, 2004.

Maxime Oquab, Leon Bottou, Ivan Laptev, and Josef Sivic. Learning and transferring mid-level image representations using convolutional neural networks. In *Proceedings of the IEEE conference on computer vision and pattern recognition*, pages 1717–1724, 2014.

Rui Pan, Hansheng Wang, and Runze Li. Ultrahigh-dimensional multiclass linear discriminant analysis by pairwise sure independence screening. *Journal of the American Statistical Association*, 111(513):169–179, 2016.

Sinno Jialin Pan and Qiang Yang. A survey on transfer learning. *IEEE Transactions on knowledge and data engineering*, 22(10):1345–1359, 2010.

Francisco Pereira, Bin Lou, Brianna Pritchett, Samuel Ritter, Samuel J Gershman, Nancy Kanwisher, Matthew Botvinick, and Evelina Fedorenko. Toward a universal decoder of linguistic meaning from brain activation. *Nature communications*, 9(1):963, 2018.

David W. Scott. *Multivariate Density Estimation: Theory, Practice, and Visualization*. Wiley, 1992.

Claude E. Shannon. A Mathematical Theory of Communication. *Bell System Technical Journal*, 27(3):379–423, 1948.

Ali Sharif Razavian, Hossein Azizpour, Josephine Sullivan, and Stefan Carlsson. CNN features off-the-shelf: an astounding baseline for recognition. In *Proceedings of the IEEE conference on computer vision and pattern recognition workshops*, pages 806–813, 2014.

Efstathios Stamatatos, Walter Daelemans, Ben Verhoeven, Patrick Juola, Aurelio López-López, Martin Potthast, and Benno Stein. Overview of the author identification task at PAN 2014. In *CLEF (Working Notes)*, pages 877–897, 2014.

Roberto Togneri and Daniel Pullella. An overview of speaker identification: Accuracy and robustness issues. *IEEE Circuits and Systems Magazine*, 11(2):23–61, 2011.

Jason Weston and Chris Watkins. Support vector machines for multi-class pattern recognition. In *ESANN*, volume 99, pages 219–224, 1999.

Wing H Wong and Li Ma. Optional Pólya tree and Bayesian inference. *The Annals of Statistics*, 38(3):1433–1459, 2010.